Articles

Redox-Induced Terpyridyl Substitution in the Os(VI)−Hydrazido Complex, *trans*-$[Os^{VI}(tpy)(Cl)_2(NN(CH_2)_4O)]^{2+}$

My Hang V. Huynh,*,‖ Donald G. Lee,† Peter S. White,# and Thomas J. Meyer*,§

Department of Chemistry, Venable and Kenan Laboratories,
The University of North Carolina at Chapel Hill, Chapel Hill, North Carolina 27599-3290,
and Chemistry Division, MS J514, Los Alamos National Laboratory, Los Alamos, New Mexico 87545

Received October 18, 2000

Reaction between the Os(VI)−hydrazido complex, *trans*-$[Os^{VI}(tpy)(Cl)_2(NN(CH_2)_4O)]^{2+}$ (tpy = 2,2′:6′,2″-terpyridine and $O(CH_2)_4N^-$ = morpholide), and a series of N- or O-bases gives as products the substituted Os(VI)−hydrazido complexes, *trans*-$[Os^{VI}(4'\text{-}RNtpy)(Cl)_2(NN(CH_2)_4O)]^{2+}$ or *trans*-$[Os^{VI}(4'\text{-}ROtpy)(Cl)_2(NN(CH_2)_4O)]^{2+}$ (RN^- = anilide ($PhNH^-$); *S*,*S*-diphenyl sulfilimide ($Ph_2S{=}N^-$); benzophenone imide ($Ph_2C{=}N^-$); piperidide ($(CH_2)_5N^-$); morpholide ($O(CH_2)_4N^-$); ethylamide ($EtNH^-$); diethylamide (Et_2N^-); and *tert*-butylamide (*t*-$BuNH^-$) and RO^- = *tert*-butoxide (*t*-BuO^-) and acetate ($MeCO_2^-$). The rate law for the formation of the morpholide-substituted complex is first order in *trans*-$[Os^{VI}(tpy)(Cl)_2(NN(CH_2)_4O)]^{2+}$ and second order in morpholine with k_{morp}(25 °C, CH_3CN) = (2.15 ± 0.04) × 10^6 M^{-2} s^{-1}. Possible mechanisms are proposed for substitution at the 4′-position of the tpy ligand by the added nucleophiles. The key features of the suggested mechanisms are the extraordinary electron withdrawing effect of Os(VI) on tpy and the ability of the metal to undergo intramolecular Os(VI) to Os(IV) electron transfer. These substituted Os(VI)−hydrazido complexes can be electrochemically reduced to the corresponding Os(V), Os(IV), and Os(III) forms. The Os−N bond length of 1.778(4) Å and Os−N−N angle of 172.5(4) ° in *trans*-$[Os^{VI}(4'\text{-}O(CH_2)_4Ntpy)(Cl)_2(NN(CH_2)_4O)]^{2+}$ are consistent with sp-hybridization of the α-nitrogen of the hydrazido ligand and an Os−N triple bond. The extensive ring substitution chemistry implied for the Os(VI)−hydrazido complexes is discussed.

Introduction

We recently identified a novel series of reactions between the Os(VI)−hydrazido complex, *trans*-$[Os^{VI}(tpy)(Cl)_2(NN(CH_2)_4O)]^{2+}$ (**1**), and N− or O-bases in which nucleophilic substitution occurs at the 4′-position of the tpy ligand accompanied by internal electron transfer.[1] In this manuscript, we extend the initial observation and provide further elaboration on the redox chemistry of the substituted products.

Experimental Section

The following complexes and salts appear in this study: *trans*-$[Os^{VI}(tpy)(Cl)_2(NN(CH_2)_4O)](PF_6)_2$ (**1**); *trans*-$[Os^{VI}(tpy)(Cl)_2(N)](PF_6)$ (**2**); *trans*-$[Os^{V}(tpy)(Cl)_2(NN(CH_2)_4O)](PF_6)$ (**3**); *trans*-$[Os^{VI}(4'\text{-}O(CH_2)_4Ntpy)(Cl)_2(NN(CH_2)_4O)](PF_6)_2$ (**4**); *trans*-$[Os^{V}(4'\text{-}O(CH_2)_4Ntpy)(Cl)_2(NN(CH_2)_4O)](PF_6)$ (**5**); *cis*-$[Os^{IV}(4'\text{-}O(CH_2)_4Ntpy)(Cl)(NCCH_3)(NN(CH_2)_4O)](PF_6)$ (**6**); *cis*-$[Os^{III}(4'\text{-}O(CH_2)_4Ntpy)(Cl)(NCCH_3)(NN(CH_2)_4O)]$ (**7**).

Abbreviations and Formulas. The abbreviations and formulas used in the text include the following: tpy = 2,2′:6′,2″-terpyridine; TBAH = $[Bu_4N](PF_6)$ = tetrabutylammonium hexafluorophosphate; Ph = phenyl; Me = methyl; Et = ethyl; and *t*-Bu = *tert*-butyl.

Materials. House-distilled water was purified with a Barnstead E-Pure deionization system. High purity acetonitrile was used as received from Burdick and Jackson. Osmium tetraoxide (> 99%) was purchased from Pressure Chemical Company. Aniline, *S*,*S*-diphenyl sulfilimine, benzophenone imine, morpholine, piperidine, ethylamine, diethylamine, *tert*-butylamine, potassium *tert*-butoxide, and tetrabutylammonium acetate were purchased from Aldrich and used without further purification. Deuterated solvents were purchased from Cambridge Isotope Laboratories and used as received. TBAH was recrystallized three times from boiling ethanol and dried under vacuum at 120° C for 2 days. Other chemicals employed in the preparation of compounds were reagent grade and used without further purification.

Instrumentation and Measurement. FTIR, ^1H NMR, UV−vis, and near-IR spectra, elemental analyses, cyclic voltammetric data, and kinetic studies by UV−vis monitoring were obtained as previously described.[1,2]

The rates of rapid reactions were determined by using a Hi-Tech CU-61 rapid scanning UV−vis spectrophotometer attached to a Hi-Tech Scientific SF-61 double mixing stopped-flow apparatus. The data were analyzed with KinetAsyst 2.0 software. For all kinetic studies, the solvent was acetonitrile, and the temperature was maintained at 25.0 ± 0.1 °C by use of a Lauda RM6 circulating water bath. In each experiment, an excess of morpholine substrate was used in order to obtain pseudo-first-order kinetics. For the reaction between *trans*-$[Os^{VI}(tpy)(Cl)_2(NN(CH_2)_4O)]^{2+}$ and morpholine, the concentration of Os(VI) was 1.05 × 10^{-5} M and the concentration of morpholine was in the range of 1.04 × 10^{-4} M − 3.46 × 10^{-4} M.

Recovery of Tpy from Os(VI)−Hydrazido and Os(VI)−Nitrido Complexes. *trans*-$[Os^{VI}(tpy)(Cl)_2(N)]Cl$ (200 mg, 0.368 mmol) was

* To whom correspondence should be addressed.
§ Associate Laboratory Director for Strategic and Supporting Research, Los Alamos National Laboratory. E-mail: tjmeyer@lanl.gov. Phone: 1-505-667-8597. Fax: 1-505-667-5450.
‖ Director-Funded Postdoctoral Fellow, Chemistry Division, Los Alamos National Laboratory. E-mail: huynh@lanl.gov. Phone: 505-667-3968. Fax: 505-667-9905.
† Present address: Department of Chemistry, University of Regina, Canada. E-mail: dglee@uregina.ca.
# University of North Carolina at Chapel Hill.

(1) Huynh, M. H. V.; Lee, D. G.; White, P. S.; Meyer, T. J. *J. Am. Chem. Soc.* **1999**, *121*, 10446.

10.1021/ic001154i CCC: $20.00
Published on Web 06/28/2001

Table 1. UV−Vis and Electrochemical Data for Morpholide and Alkyl-Amide Substituted Tpy Osmium Complexes in 0.1 M TBAH/CH_3CN

salts	λ_{max}, nm ($\epsilon \times 10^3$ $M^{-1}cm^{-1}$)[a]	$E_{1/2}$ vs SSCE[b]		
		Os(VI/V)	Os(V/IV)	Os(IV/III)
trans-[Os^{VI}(tpy)$(Cl)_2$($NN(CH_2)_4O$)]$(PF_6)_2$ (**1**)	790 (0.13); 586 (0.43); 470 (2.39); 330 (21.2); 288 (25.4); 252 (35.7); 208 (44.7)	+0.980	0.000	−0.790
trans-[Os^{VI}(4-$O(CH_2)_4$Ntpy)$(Cl)_2$($NN(CH_2)_4O$)]$(PF_6)_2$ (**4**)	624 (8.60); 344 (14.6); 308 (22.8); 282 (30.6); 240 (35.2); 218 (42.7)	+0.780	+0.150	−0.480
trans-[Os^{VI}((H)(*t*-Bu)Ntpy)$(Cl)_2$($NN(CH_2)_4O$)]$(PF_6)_2$	624 (7.74); 310 (23.0); 280 (30.1); 226 (39.0); 210 (43.3)	+0.775	+0.113	−0.586
trans-[Os^{VI}(Et_2Ntpy)$(Cl)_2$($NN(CH_2)_4O$)]$(PF_6)_2$	624 (7.48); 308 (23.0); 284 (29.2); 234 (36.7); 218 (34.7)	+0.761	+0.144	−0.533
trans-[Os^{VI}($(CH_2)_5$Ntpy)$(Cl)_2$($NN(CH_2)_4O$)]$(PF_6)_2$	636 (8.83); 308 (23.3); 278 (30.1); 264 (31.2); 212 (41.1)	+0.759	+0.156	−0.580

[a] Uncertainty = ±(0.02−0.05) × 10^3 M^{-1} cm^{-1}. [b] Uncertainty = ±2 mV.

dissolved/suspended in water (8 mL), and $AgClO_4 \cdot H_2O$ (271 mg, 1.31 mmol) was added. The resulting black suspension was stirred vigorously for 2 days and then centrifuged to remove precipitated AgCl. Potassium carbonate (116 mg, 0.841 mmol) in water (34 mL) was added. The solution was stirred for a few minutes and centrifuged again to remove precipitated Ag_2CO_3. The resulting solution was dark green with a pH of 4. More potassium carbonate (300 mg) was added giving a deep red solution of higher pH. On standing, a white precipitate slowly separated and was extracted into CH_2Cl_2 (3 × 20 mL). This solution was dried over anhydrous Na_2SO_4, and the solvent evaporated (with a rotovap) to give a colorless solution. On drying under vacuum and over P_2O_5, a white solid that was later identified as the tpy ligand remained (27 mg, 0.116 mmol, 32%). The product was characterized by the use of UV−vis and ^{1}H NMR spectroscopies.

trans-[Os^{VI}(tpy)$(Cl)_2$($NN(CH_2)_4O$)]$(PF_6)_2$ (0.038 mmol) was suspended in water (10 mL), and $AgClO_4 \cdot H_2O$ (100 mg, 0.48 mmol) was added. The solution was sonicated periodically and stirred vigorously for 2 days. Water (5 mL) was added at the beginning of the second day. The dark brown/yellow solution was centrifuged to remove precipitated AgCl and other undissolved material. The precipitate was washed with water (2 × 3 mL) giving a solution of pH 4.5. Potassium carbonate (77 mg, 0.56 mmol) was added, and precipitated Ag_2CO_3 was removed by centrifuging, leaving a pale brown solution with a pH of 7. More potassium carbonate (200 mg) was added making the solution distinctly basic. This solution was stored for 1 day and then extracted repeatedly with CH_2Cl_2 (3 × 30 mL). The extract was dried over anhydrous Na_2SO_4 and concentrated on a rotary evaporator leaving a gray residue that was dried under vacuum over P_2O_5. The tpy ligand was confirmed by UV−vis and ^{1}H NMR spectroscopies.

Synthesis and Characterization. The following complexes and compounds were prepared by literature procedures: *trans*-[Os^{VI}(tpy)$(Cl)_2$($NN(CH_2)_4O$)]$(PF_6)_2$ (**1**),[2] *trans*-[Os^{VI}(tpy)$(Cl)_2$(N)](PF_6) (**2**),[3] *trans*-[Os^{V}(tpy)$(Cl)_2$($NN(CH_2)_4O$)](PF_6) (**3**).[4]

***trans*-[Os^{VI}(4′-$O(CH_2)_4$Ntpy)$(Cl)_2$($NN(CH_2)_4O$)]$(PF_6)_2$ (4).** A rapid reaction occurred when morpholine was added dropwise to **1** (electrochemically generated from **3**) as indicated by a change in color from light brown to bright blue. The amount of morpholine required to produce a complete reaction was monitored by UV−vis spectroscopy at λ_{max} = 624 nm. From cyclic voltammetry, the resulting product was determined to be a 2:1 mixture of *trans*-[Os^{V}(tpy)$(Cl)_2$($NN(CH_2)_4O$)]$^+$ and the morpholide-substituted product, *trans*-[Os^{VI}(4′-$O(CH_2)_4$Ntpy)$(Cl)_2$($NN(CH_2)_4O$)]$^{2+}$. This process was repeated two more times under an Ar atmosphere in the following order: (1) *trans*-[Os^{V}(tpy)$(Cl)_2$($NN(CH_2)_4O$)]$^+$ was oxidized to *trans*-[Os^{VI}(tpy)$(Cl)_2$($NN(CH_2)_4O$)]$^{2+}$ at E_{app} = 1.23 V and (2) morpholine was added to the solution mixture dropwise until the absorbance at λ_{max} = 624 nm remained constant. Yield is in the range of 90−95% under Ar atmosphere. Anal. Calcd for $OsC_{23}H_{26}Cl_2N_6O_2P_2F_{12} \cdot 0.2$ [Bu_4N](PF_6): C, 30.06; H, 3.20; N, 8.29. Found: C, 30.42; H, 3.19; N, 8.51. ^{1}H NMR (δ, CD_3CN): eleven aromatic protons for the tpy ligand appear at 8.63−8.40 ppm (5 protons at positions **1** in Scheme 1), 8.27−8.15 ppm (2 protons at positions **2** in Scheme 1), 8.11−7.97 ppm (4 protons at positions **3** in Scheme 1). Eight aminoalkyl protons are not equivalent with resonances appearing at 2.85, 3.85, 4.45, and 5.05 ppm.

Scheme 1

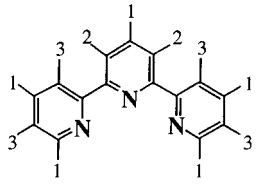

Crystals of **4** were grown by a slow diffusion of Et_2O with a stream of Ar into a solution containing **4**, prepared as described above. UV−vis spectroscopic and cyclic voltammetric data of *trans*-[Os^{VI}(4′-$O(CH_2)_4$Ntpy)$(Cl)_2$($NN(CH_2)_4O$)]$(PF_6)_2$ in CH_3CN are summarized in Table 1.

***cis*-[Os^{IV}(4′-$O(CH_2)_4$Ntpy)(Cl)($NCCH_3$)($NN(CH_2)_4O$)]$^+$ (6) and *cis*-[Os^{III}(4′-$O(CH_2)_4$N-tpy)(Cl)($NCCH_3$)($NN(CH_2)_4O$)] (7).** Compounds **6** and **7** were electrochemically generated from **4** in 0.1 M TBAH/CH_3CN at E_{app} = −0.100 V and −0.720 V, respectively. Reminiscent of the reduction of **3**, the reduction to **6** was also accompanied by solvolysis and isomerization. As a consequence, the cis configuration and the solvolyzed solvento ligand in **6** remain in **7**.[5]

X-ray Structural Determinations. Crystal data, intensity collection information, and structure refinement parameters for the structure of **4** are listed in Table 2. The structure was solved by direct methods. The non-hydrogen atoms were located in subsequent difference Fourier maps. Empirical absorption corrections were applied with SADABS. The ORTEP plotting program was used to generate the structure shown in Figure 1.[6] Hydrogen atoms were included in calculated positions with thermal parameters derived from the atom to which they were bonded. All computations were performed by using the NRCVAX suite of programs.[7] Atomic scattering factors were taken from a standard source[8] and corrected for anomalous dispersion. The final positional parameters along with their standard deviations as estimates from the inverse matrix, tables of hydrogen atom parameters, anisotropic thermal parameters, and observed/calculated structure amplitudes for **4** are available as Supporting Information Materials. Selected bond lengths and angles for the cation are listed in Tables 3 and 4, respectively.

(2) (a) Huynh, M. H. V.; El-Samanody, E.-S.; Demadis, K. D.; White, P. S.; Meyer, T. J. *Inorg. Chem.* **2000**, *39*, 3075. (b) Huynh, M. H. V.; El-Samanody, E.-S.; Meyer, T. J.; White, P. S. *Inorg. Chem.* **1999**, *38*, 3760.

(3) (a) Ware, D. C.; Taube, H. *Inorg. Chem.* **1991**, *30*, 4598. (b) Pipes, D. W.; Bakir, M.; Vitols, S. E.; Hodgson, D. J.; Meyer, T. J. *J. Am. Chem. Soc.* **1990**, *112*, 5507.

(4) (a) Huynh, M. H. V.; El-Samanody, E.-S.; Demadis, K. D.; White, P. S.; Meyer, T. J. *J. Am. Chem. Soc.* **1999**, *121*, 1403. (b) Huynh, M. H. V.; White, P. S.; Meyer, T. J. *J. Am. Chem. Soc.* **1999**, *121*, 4530.

(5) Huynh, M. H. V.; White, P. S.; Meyer, T. J. Manuscript in preparation.

(6) Johnson, C. K. *ORTEP: A Fortran Thermal Ellipsoid Plot Program*; Technical Report ORNL-5138; Oak Ridge National Laboratory: Oak Ridge, TN, 1976.

(7) Gabe, E. J.; Le Page, Y.; Charland, J.-P.; Lee, F. L.; White, P. S. *J. Appl. Crystallogr.* **1989**, *22*, 384.

(8) *International Tables for X-ray Crystallography*; Kynoch Press: Birmingham, U.K., 1974; Vol. IV.

Table 2. Summary of Crystal Data, Intensity Collection, and Structure Refinement Parameters for *trans*-$[Os^{VI}(4\text{-}O(CH_2)_4Ntpy)(Cl)_2(NN(CH_2)_4O)]^{2+}$

salt	**4**	collection temperature	−100 °C
formula	$OsC_{23}H_{26}N_6Cl_2O_2P_2F_6$	abs. coefficient μ, mm^{-1}	4.39
molecular weight	969.52	$F(000)$	1880.05
a (Å)	8.4693(5)	$2\theta_{max}$ (deg)	50.0
b (Å)	20.2029(11)	total reflections	19361
c (Å)	18.6137(10)	unique reflections	5609
β (Å)	94.768(1)	refined reflections	4149
V (Å^3)	3173.9(3)	merging R value	0.041
Z	4	number of parameters	433
crystal system	monoclinic	R (%)[a]	0.047
space group	$P2_1/c$	R_w (%)[b]	0.065
crystal size (mm)	0.25 × 0.10 × 0.10	goodness of fit[c]	0.000
d_{calcd} (g/cm^3)	2.029	deepest hole (e/Å^3)	−1.000
diffractometer	Siemens CCD Smart	highest peak (e/Å^3)	1.310
radiation	Mo Kα (λ = 0.71073 Å)	σ	0.001

[a] $R = \sum(|F_o - F_c|)/\sum|F_o|$. [b] $R_w = [\sum(w|F_o - F_c|)^2/\sum w(F_o)^2]^{1/2}$. [c] GoF = $[\sum w(F_o - F_c)^2/(\text{no. of reflections} - \text{no. of parameters})]^{1/2}$.

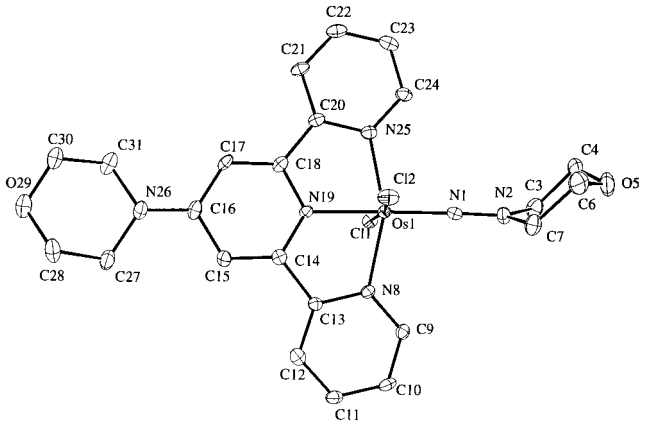

Figure 1. ORTEP diagrams (30% ellipsoids) and labeling scheme for the cation *trans*-$[Os^{VI}(4'\text{-}O(CH_2)_4Ntpy)(Cl)_2(NN(CH_2)_4O)]^{2+}$.

Table 3. Bond Lengths (Å) for *trans*-$[Os^{VI}(4\text{-}O(CH_2)_4Ntpy)(Cl)_2(NN(CH_2)_4O)]^{2+}$

Os(1)−Cl(1)	2.3258(14)	C(10)−C(11)	1.377(8)	C(23)−C(24)	1.383(9)
Os(1)−Cl(2)	2.3727(14)	C(11)−C(12)	1.376(8)	C(24)−C(25)	1.347(7)
Os(1)−N(1)	1.778(4)	C(12)−C(13)	1.381(8)	N(26)−C(27)	1.478(8)
Os(1)−N(8)	2.076(4)	C(13)−C(14)	1.491(8)	N(26)−C(31)	1.484(8)
Os(1)−N(19)	1.988(4)	C(14)−C(15)	1.367(7)	C(27)−C(28)	1.530(9)
Os(1)−N(25)	2.077(5)	C(14)−C(19)	1.338(7)	C(28)−O(29)	1.441(9)
N(1)−N(2)	1.237(6)	C(15)−C(16)	1.428(8)	O(29)−C(30)	1.406(8)
N(2)−C(3)	1.492(8)	C(16)−C(17)	1.429(8)	C(30)−C(31)	1.511(9)
N(2)−C(7)	1.493(7)	C(16)−N(26)	1.353(7)	C(22)−C(23)	1.375(9)
C(3)−C(4)	1.515(9)	C(17)−C(18)	1.372(8)	C(9)−C(10)	1.379(8)
C(4)−O(5)	1.403(9)	C(18)−N(19)	1.372(7)	C(21)−C(22)	1.369(9)
O(5)−C(6)	1.412(10)	C(18)−C(20)	1.465(8)	N(8)−C(13)	1.368(7)
C(6)−C(7)	1.519(9)	C(20)−C(21)	1.375(8)	C(20)−N(25)	1.369(7)
N(8)−C(9)	1.347(7)				

Results

Reactions of the Os(VI)−Hydrazido Complexes. A series of reactions occurs between **1** and nucleophiles including $PhCH_2OH$, $HPPh_2$, PPh_3, SPh_2, SEt_2, Na(OMe), K(OEt), $HNPh_2$, $NPhMe_2$, NEt_3, and NPh_3, for which there is no evidence for tpy ring attack. The results of these studies for $PhCH_2OH$, PPh_3, SPh_2, and SEt_2 are reported in the previous manuscript.[5] For the reaction between **1** and benzyl alcohol, net hydride transfer was observed. With PPh_3, a net double Cl atom transfer occurred presumably followed by hydrolysis of Cl_2PPh_3 by a trace of H_2O to give $OPPh_3$ and *cis*-$[Os^{IV}(tpy)(NCCH_3)_2(NN(CH_2)_4O)]^{2+}$.

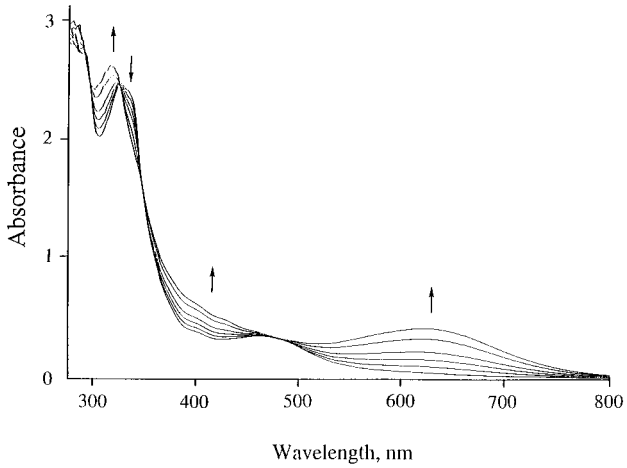

Figure 2. Spectral changes upon sequential addition of aliquots of 5.0×10^{-6} M $HN(CH_2)_4O$ in CH_3CN to 1.0×10^{-6} M *trans*-$[Os^{VI}(tpy)(Cl)_2(NN(CH_2)_4O)]^{2+}$ in CH_3CN.

For the sulfides and alkoxides, electron transfer occurs to give Os(V). For secondary and tertiary arylamines, electron-transfer results in oxidative coupling, with NMe_2Ph to give $[Me_2NPh\text{-}PhNMe_2](PF_6)_2$.[9]

Ring Substitution. Upon addition of morpholine to electrochemically generated **1** in CH_3CN, a rapid reaction occurs as shown by a change in color from light brown to bright blue. UV−vis spectral changes with incremental additions of morpholine are shown in Figure 2. Cyclic voltammetry at the end of the first stage, Figure 3A, revealed two sets of waves: (1) three reversible couples, denoted with stars, at $E_{1/2} = +0.78$ V (Os(VI/V)), +0.15V (Os(V/IV)), and −0.48V (Os(IV/III)) and (2) two additional reversible couples at $E_{1/2} = +0.98$ V (Os(VI/V)) and 0.00 V (Os(V/IV)) in 0.1 M TBAH/CH_3CN (versus SSCE). The cyclic voltammogram of *trans*-$[Os^{V}(tpy)(Cl)_2(NN(CH_2)_4O)]^{+}$ (**3**) recorded under the same conditions is shown in Figure 3B for comparison. From relative peak currents, the product ratio of **3**:**4** was 2:1. On the basis of these results, the stoichiometry of the reaction is as shown in eq 1.

$$3\ \textit{trans}\text{-}[Os^{VI}(tpy)(Cl)_2(NN(CH_2)_4O)]^{2+} + 3\ HN(CH_2)_4O \rightarrow \textit{trans}\text{-}[Os^{VI}(4'\text{-}O(CH_2)_4Ntpy)(Cl)_2(NN(CH_2)_4O)]^{2+} + 2\ H_2N(CH_2)_4O^{+} + 2\ \textit{trans}\text{-}[Os^{V}(tpy)(Cl)_2(NN(CH_2)_4O)]^{+} \quad (1)$$

The reaction was analyzed further by cyclic voltammetry at different stages following incremental additions of morpholine. Before morpholine was added, the only Os(VI/V) wave observed was for *trans*-$[Os^{VI}(tpy)(Cl)_2(NN(CH_2)_4O)]^{2+/+}$ at $E_{1/2} = +0.98$ V (Figure 4A). After addition of $^1/_3$ equiv of morpholine (relative to Os(VI)), waves appeared at $E_{1/2} = +0.98$ V and $E_{1/2} = +0.78$ V for the Os(VI/V) couples of **3** and **4**, respectively. The peak current ratio was 2:1 (Figure 4B). The solution mixture was reoxidized at $E_{app} = 1.23$ V (versus SSCE). After repeating the addition of morpholine, the ratio of **3** to **4** in the solution mixture was approximately 1:2 (Figure 4C). Further addition of morpholine after the second reoxidation cycle resulted in nearly quantitative formation of **4** based on peak current ratios (Figure 4D). The results of this experiment showed that ring addition of the amine could be made quantitative by reoxidizing the Os-

(9) Huynh, M. H. V.; White, P. S.; Meyer, T. J. Unpublished results.

Table 4. Angles (deg) for *trans*-[Os^{VI}(4-$O(CH_2)_4$Ntpy)$(Cl)_2(NN(CH_2)_4O)]^{2+}$

Cl(1)−Os(1)−Cl(2)	172.22(5)	C(23)−C(24)−N(25)	121.9(5)	O(5)−C(6)−C(7)	110.3(6)
Cl(1)−Os(1)−N(1)	96.99(14)	Os(1)−N(25)−C(20)	114.0(4)	N(2)−C(7)−C(6)	107.5(5)
Cl(1)−Os(1)−N(8)	89.21(12)	OS(1)−N(25)−C(24)	126.8(4)	Os(1)−N(8)−C(9)	126.9(4)
Cl(1)−Os(1)−N(19)	87.71(13)	C(20)−N(25)−C(24)	119.2(5)	OS(1)−N(8)−C(13	114.9(3)
Cl(1)−Os(1)−N(25)	88.42(13)	C(16)−N(26)−C(27)	122.7(5)	C(9)−N(8)−C(13)	118.2(5)
Cl(2)−Os(1)−N(1)	90.37(14)	C(16)−N(26)−C(31)	123.0(5)	N(8)−C(9)−C(10)	122.6(5)
Cl(2)−Os(1)−N(8)	91.94(12)	C(27)−N(26)−C(31)	113.2(4)	C(9)−C(10)−C(11)	118.9(5)
Cl(2)−Os(1)−N(19)	85.01(13)	N(26)−C(27)−C(28)	110.5(5)	C(10)−C(11)−C(12)	119.4(5)
Cl(2)−Os(1)−N(25)	87.56(13)	C(27)−C(28)−O(29)	110.5(5)	C(11)−C(12)−C(13)	119.7(5)
N(1)−Os(1)−N(8)	100.39(18)	C(28)−O(29)−C(30)	109.8(4)	N(8)−C(13)−C(12)	121.2(2)
N(1)−Os(1)−N(19)	175.06(19)	O(29)−C(30)−C(31)	112.0(5)	N(8)−C(13)−(14)	114.3(5)
N(1)−Os(1)−N(25)	102.31(19)	N(26)−C(31)−C(30)	110.7(5)	C(12)−C(13)−C(14)	124.4(5)
N(8)−Os(1)−N(19)	78.10(17)	N(2)−C(3)−C(4)	105.7(5)	C(13)−C(14)−C(15)	125.8(5)
N(8)−Os(1)−N(25)	157.30(17)	C(3)−C(4)−O(5)	109.4(5)	C(13)−C(14)−N(19)	112.3(4)
N(19)−Os(1)−N(25)	79.25(18)	C(4)−O(5)−C(6)	110.5(5)	C(15)−C(14)−N(19)	121.9(5)
Os(1)−N(1)−N(2)	172.5(4)	Os(1)−N(19)−C(18)	118.1(3)	C(14)−C(15)−C(16)	119.1(5)
N(1)−N(2)−C(3)	120.9(5)	C(14)−N(19)−C(18)	121.5(4)	C(15)−C(16)−C(17)	117.6(5)
N(1)−N(2)−C(7)	120.6(5)	C(18)−C(20)−C(21)	123.9(5)	C(15)−C(16)−N(26)	120.6(5)
C(3)−N(2)−C(7)	118.5(4)	C(17)−C(16)−N(26)	121.8(5)	Os(1)−N(19)−C(14)	120.4(4)
C(18)−C(20)−N(25)	115.5(5)	C(16)−C(17)−C(18)	120.0(5)	C(22)−C(23)−C(24)	118.3(5)
C(21)−C(20)−N(25)	120.6(5)	C(17)−C(18)−N(19)	119.9(5)	C(20)−C(21)−C(22)	119.6(5)
C(17)−C(18)−C(20)	126.9(5)	C(21)−C(22)−C(23)	120.5(6)	N(19)−C(18)−C(20)	113.2(5)

(V) formed in eq 1 to Os(VI). Under these conditions, the net reaction is shown in eq 2.

$$3\ \textit{trans}\text{-}[Os^{VI}(tpy)(Cl)_2(NN(CH_2)_4O)]^{2+} + 3\ HN(CH_2)_4O \xrightarrow{-6e^-} 3\ \textit{trans}\text{-}[Os^{VI}(4'\text{-}O(CH_2)_4Ntpy)(Cl)_2 - (NN(CH_2)_4O)]^{2+} + 6\ H^+ \quad (2)$$

The morpholide-substituted Os(VI)−hydrazido complex was isolated and fully characterized by X-ray crystallography (Figure 1), elemental analysis, cyclic voltammetry, and ^{1}H NMR and UV−vis spectroscopies. On the basis of the cyclic voltammetric data in Figure 3, reversible couples appear at +0.78 V, +0.15 V, and −0.48 V (denoted with stars in Figure 3A) for the Os(VI/V), Os(V/IV), and Os(IV/III) couples of *trans*-[Os^{VI}(4′-$O(CH_2)_4$Ntpy)$(Cl)_2(NN(CH_2)_4O)]^{2+}$. Reminiscent of the reduction of **1**, reduction of the morpholide-substituted complex to Os(IV) was also accompanied by solvolysis and isomerization.[5] Electronic spectra of oxidation states VI to III for the substituted complex are shown in Figure 5.

The kinetics of the reaction between **1** and morpholine were studied by stopped-flow mixing with UV−vis monitoring. A large excess of morpholine (1.04×10^{-4} to 3.45×10^{-4} M) was used to obtain pseudo-first-order kinetic conditions. A plot of k_{obs} versus $[HN(CH_2)_4O)]^2$ was linear consistent with kinetics second order in morpholine (Supporting Information, Figure 1) and the rate law in eqs 3 and 4:

$$\frac{-d[Os^{VI}(tpy)(Cl)_2(NN(CH_2)_4O)]^{2+}}{dt} = k_{morp}\,[Os^{VI}(tpy)(Cl)_2(NN(CH_2)_4O)]^{2+}\,[HN(CH_2)_4O]^2 \quad (3)$$

$$= k_{obs}\,[Os^{VI}(tpy)(Cl)_2(NN(CH_2)_4O)]^{2+} \quad (4)$$

with $k_{obs} = k_{morp}\,[HN(CH_2)_4O]^2$ and $k_{morp} = (2.15 \pm 0.04) \times 10^6\ M^{-2}\ s^{-1}$.

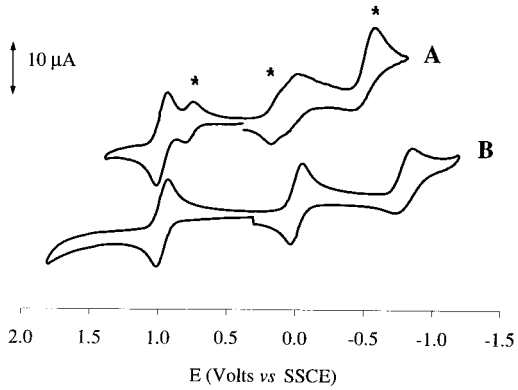

Figure 3. (A) Cyclic voltammogram after mixing *trans*-[Os^{VI}(tpy)$(Cl)_2(NN(CH_2)_4O)](PF_6)_2$ (3.8×10^{-3} M) and $HN(CH_2)_4O$ (1.3×10^{-3} M) in 0.1 M TBAH/CH_3CN vs SSCE. The stars (*) label waves that arise from **5** produced in the reaction. (B) Cyclic voltammogram of *trans*-[Os^{V}(tpy)$(Cl)_2(NN(CH_2)_4O)](PF_6)$ as in **A**, showing the chemically reversible waves for the Os(VI/V), Os(V/IV), and Os(IV/III) couples at $E_{1/2} = +0.98$ V, 0.00 V, and −0.79 V ($E_{1/2} = (E_{p,a} + E_{p,c})/2$).

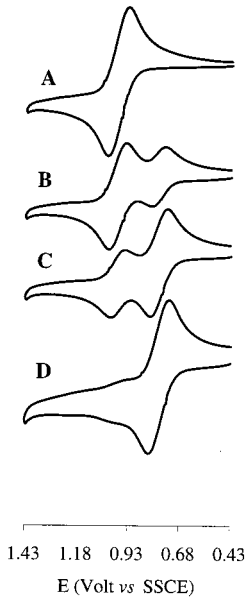

Figure 4. (A) Cyclic voltammogram of *trans*-[Os^{VI}(tpy)$(Cl)_2(NN(CH_2)_4O)](PF_6)_2$ (3.8×10^{-3} M) in 0.1 M TBAH/CH_3CN vs SSCE in the potential region for the Os(VI/V) couples. (B) Cyclic voltammogram of the reaction mixture after the first addition of $HN(CH_2)_4O$ (1.3×10^{-3} M). (C) Cyclic voltammogram after the first reoxidation at $E_{app} = 1.23$ V (versus SSCE) and the second addition of $HN(CH_2)_4O$. (D) Cyclic voltammogram after the second reoxidation and the third addition of $HN(CH_2)_4O$.

Table 5. Internal Ligand Charge Transfer (ILCT) (or Ligand-to-Metal Charge Transfer (LMCT)) Bands and Reduction Potentials for the Adducts from Reactions between *trans*-$[Os^{VI}(tpy)(Cl)_2(NN(CH_2)_4O)]^{2+}$ and N- or O-Bases in CH_3CN

		$E_{1/2}$ (Volts vs SSCE)[b]		
base	λ_{max} (nm)[a]ILCT	Os(VI/V)	Os(V/IV)	Os(IV/III)
none (*trans*-$[Os^{VI}(tpy)(Cl)_2(NN(CH_2)_4O)]^{2+}$)	624	0.980	0.000	−0.790
K(O-*t*-Bu)	N.O.[c]	0.790	0.135	−0.590
$HN(CH_2)_4O$	624	0.780	0.150	−0.480
H_2NEt	604	0.779	0.094	−0.490
(2,4,6-*t*-Bu)$_3$py	614	0.779	0.110	−0.497
(4-*t*-Bu)py[d]	590	0.776	0.161	−0.550
H_2N(*t*-Bu)[e]	624	0.775	0.113	−0.586
$HN{=}CPh_2$	594	0.775	0.155	−0.502
$NH_4(OC(O)CH_3)$	N.O.	0.766	0.136	−0.616
$HNEt_2$	624	0.761	0.144	−0.533
$HN(CH_2)_5$	636	0.759	0.156	−0.580
$HN{=}SPh_2$	630	0.754	0.137	−0.597
H_2NPh	660	0.568	0.163	−0.514

[a] Uncertainty = ± 2 nm. [b] Uncertainty = ± 2 mV. [c] N.O. = not observed. [d] $E_{1/2}$(*t*-Bupy)$^{+/0}$ = −1.01 V (versus SSCE). [e] $E_{1/2}$(2,4,6-Me$_3$py)$^{+/0}$ = −0.87 V (versus SSCE).

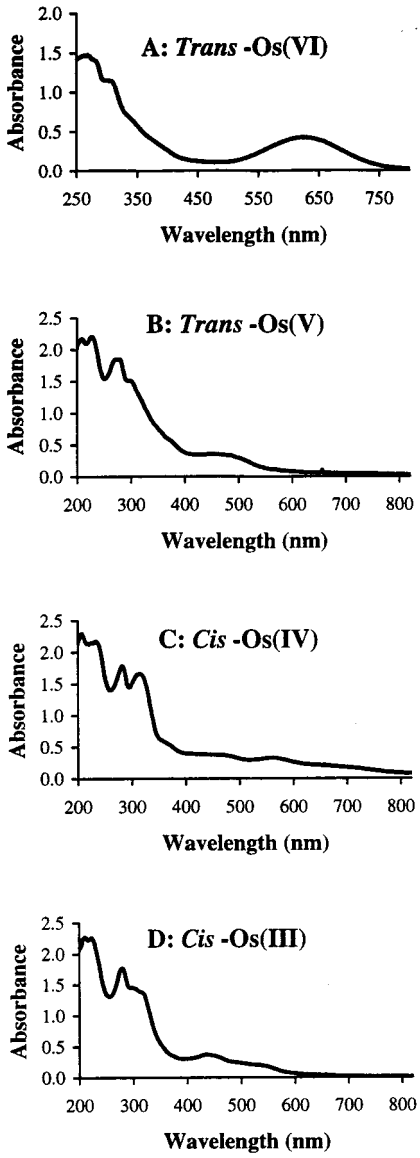

Figure 5. Absorption spectra in CH_3CN: (A) *trans*-$[Os^{VI}(4'\text{-}O(CH_2)_4\text{-}Ntpy)(Cl)_2(NN(CH_2)_4O)]^{2+}$; (B) *trans*-$[Os^{V}(4'\text{-}O(CH_2)_4Ntpy)(Cl)_2(NN(CH_2)_4O)]^{+}$; (C) *cis*-$[Os^{IV}(4'\text{-}O(CH_2)_4Ntpy)(Cl)(NCCH_3)(NN(CH_2)_4O)]^{+}$; (D) *cis*-$[Os^{III}(4'\text{-}O(CH_2)_4Ntpy)(Cl)(NCCH_3)(NN(CH_2)_4O)]$. Os(IV) and Os(III) were electrochemically generated from Os(V) in 0.1 M TBAH.

Similar ring-substitution reactions occur between **1** and other N- and O-nucleophiles including primary and secondary aliphatic amines, primary aromatic amines, bulky alkoxides, and imides. Reduction potentials and λ_{max} values for new visible absorption bands that appear for these products formed by electrochemical generation are listed in Table 5. From the data in this table, each of the products has three reversible couples at potentials near to those of the morpholide-substituted Os−hydrazido complex. No attempt was made to isolate the products.

H/D Exchange at Tpy in *trans*-$[Os^{VI}(tpy)(Cl)_2(NN(CH_2)_4O)]^{2+}$. Isotopic hydrogen exchange at the tpy ligand was investigated by ^{1}H NMR spectroscopy in CD_3CN/H_2O-D_2O mixtures. The addition of one drop of D_2O (pH = 8.47) to 0.8 mL of a CD_3CN solution containing **1** resulted in a complete exchange of H for D within 10 s as evidenced by the disappearance of all aromatic protons from 7.97 to 8.63 ppm in the ^{1}H NMR spectrum. When this experiment was repeated with H_2O (pH = 6.34), the ^{1}H NMR spectrum remained unchanged.

The ease of exchange depends on the position of the protons on the pyridyl rings, designated as **1**, **2**, and **3** in Scheme 1. As shown in Figure 6A, the aromatic protons of tpy appear in three regions: 8.63−8.40 ppm (5 H, position **1**), 8.27−8.15 ppm (2 H, position **2**), and 8.11−7.97 ppm (4 H, position **3**). When approximately equal amounts of H_2O and then D_2O as a limiting reagent compared to the complex were added to a sample of **1** in a NMR tube, the resonances of the most acidic protons at positions **1** in Scheme 1 underwent exchange, Figure 6B. As additional D_2O was added, the twin doublet resonances for the protons at positions **2** underwent exchange, Figure 6C, followed by the exchange of the protons at positions **3**.

Structure and Bonding. An ORTEP diagram of **4** is shown in Figure 1. The crystal contains discrete *trans*-$[Os^{VI}(4'\text{-}O(CH_2)_4Ntpy)(Cl)_2(NN(CH_2)_4O)]^{2+}$ cations and PF_6^- anions. The chloride ligands remain in the trans configuration in the product. Due to the structural trans effect of the nitrido ligand in the Os(VI)−nitrido complex, the middle Os−N(tpy) bond is the longest of the three rather than the shortest.[11] There is no evidence for a structural trans effect in **4**.[1] The Os−Cl bond lengths are 2.3258(14) Å and 2.3727(14) Å, nearly the same as in the parent hydrazido complex: i.e., 2.3193(22) and 2.3472(23) Å. The $N_\alpha-N_\beta$ bond length of 1.237 (6) Å lies within the normal range for hydrazido ligands (1.21(2)−1.296(11) Å).[11] The N(tpy)−Os−N(hydrazido) angle is approximately linear at

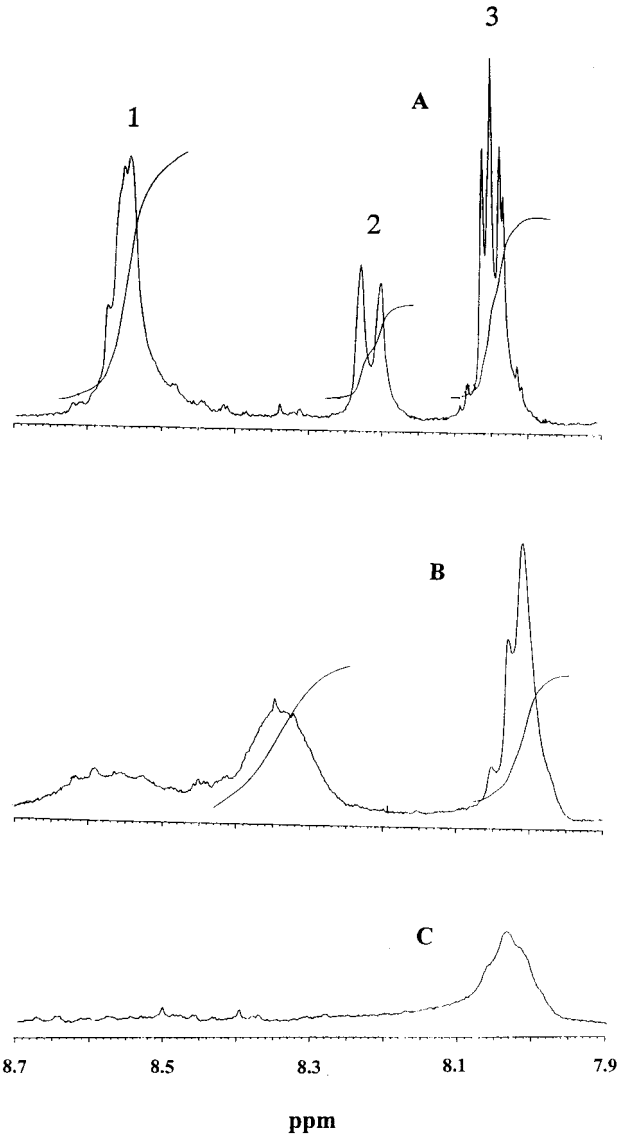

Figure 6. ^{1}H NMR spectra of an 0.8 mL CD_3CN solution containing **1**: (A) *trans*-$[Os^{VI}(tpy)(Cl)_2(NN(CH_2)_4O)]^{2+}$; (B) A after addition of 1 drop of H_2O (pH = 6.34) and then one drop of D_2O (pH = 8.47); (C) B after 2 additional drops of D_2O.

175.06(19) °. The Os−N_α−N_β angle of 172.5(4) ° indicates sp-hybridization at N_α, and the Os−N bond length of 1.778 (4) Å is consistent with triple bonding between Os(VI) and N_α.[11] Electron−electron repulsion associated with this bond contributes to the Cl−Os−Cl angle of 172.22(5)° and the bending away from the Os−N bond.

Discussion

The initially surprising observation in this work was the appearance of ring-substituted products when **1** was treated with a series of N- or O-based nucleophiles, Table 5. This reactivity is remarkable because it occurs under mild conditions and is quite general for N- and O-based nucleophiles. The net reaction is reminiscent of the Chichibabin[12] and vicarious nucleophilic substitution reactions;[13] however, they require vigorous conditions and occur only in very strong base, usually at elevated temperatures.

H/D Exchange. An equally remarkable observation, that relates to the mechanism of ring attack, is the appearance of rapid isotopic exchange of the aromatic tpy hydrogens when **1** is treated with D_2O under mild conditions in CH_3CN.[1] The observation of proton exchange for deuterium in the coordinated tpy ligand described here appears to be the first example in the literature of aromatic proton exchange in pyridyl or polypyridyl ligands under mild conditions. The facile exchange reaction points to C−H(pyridyl) bonds that are remarkably acidic. A possible mechanism, shown in eq 5, involves an initial acid−base equilibrium. The reverse reaction with the deprotonated form captured by D_2O (or HDO) would explain H/D exchange on the pyridyl rings. It seems clear that Os(VI) as an activating "substituent" is the key to facile H/D exchange.

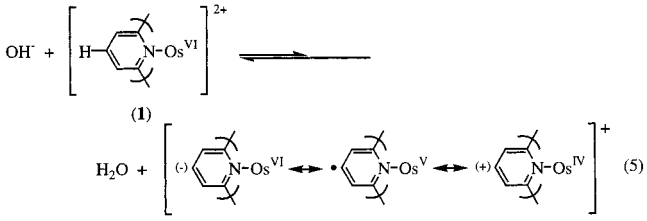

As implied by the limiting resonance structures in eq 5, a contributing factor may be the ability of Os(VI) to stabilize a carbanion intermediate by acting as an electron acceptor through orbital mixing. In any case, Os(VI) is a remarkable electron withdrawing substituent.

Ring Substitution. Although no attempt was made to obtain quantitative comparisons among the various nucleophiles, all ring additions were rapid. The kinetics of the reaction between morpholine and **1** revealed a rate law second order in base with $k_{morp} = (2.15 \pm 0.04) \times 10^6\ M^{-2}\ s^{-1}$.

Addition to the ring can be described as oxidatively induced substitution. Important features of the mechanism appear to be the bond polarization implied in eq 5 and intramolecular, two-electron-transfer based on the Os(VI/IV) couple.

The reaction is likely initiated by nucleophilic attack of the added base on the central pyridyl ring of tpy (reaction a in Scheme 2), followed by one of two rate-limiting steps: (i) proton loss to a second molecule of base (reaction b), followed by intramolecular electron transfer and further proton release (reaction c) or (ii) intramolecular two-electron-transfer induced by proton loss to a second base molecule (reaction b′) followed by rapid proton loss. Both mechanisms are consistent with the observed rate law if the initial nucleophilic addition is a rapid pre-equilibrium. However, reaction b′, which involves carbon−hydrogen bond cleavage, is the more likely candidate as a rate-limiting step.

To complete the mechanism and explain the final product distribution, it is necessary to invoke sequential oxidation of the initially formed Os(IV) product by unreacted Os(VI) (reaction d). From the reduction potentials in Table 1, $\Delta G° = -0.83$ eV for oxidation of Os(IV) by *trans*-Os(VI) to give Os-

(10) Huynh, M. H. V.; White, P. S.; Meyer, T. J. Unpublished results: (a) With the *trans effect* of the nitrido ligand in *trans*-$[Os^{VI}(tpy)(Cl)_2(N)]^+$, the middle Os−N(tpy) bond is the longest, i.e., Os−N(tpy) = 2.091(3) Å, 2.173(3) Å, and 2.098(3) Å. (b) Without the *trans effect* of the nitrido ligand in *cis*-$[Os^{VI}(tpy)(Cl)_2(N)]^+$, the middle Os−N(tpy) bond is the shortest as is normal, i.e., Os−N(tpy) = 2.089(4) Å, 2.007-(4) Å, and 2.085(4) Å.

(11) Kahlal, S.; Saillard, J.-Y.; Hamom, J.-R.; Manzur, C.; Carrillo, D. *J. Chem. Soc., Dalton Trans.* **1998**, 1229 and references therein.

(12) McGill, C. K.; Rappa, A. *Adv. Heterocycl. Chem.* **1988**, *44*, 1.

(13) Makosza, M.; Stalinski, K. *Polish J. Chem.* **1999**, *73*, 151 and references therein.

Scheme 2

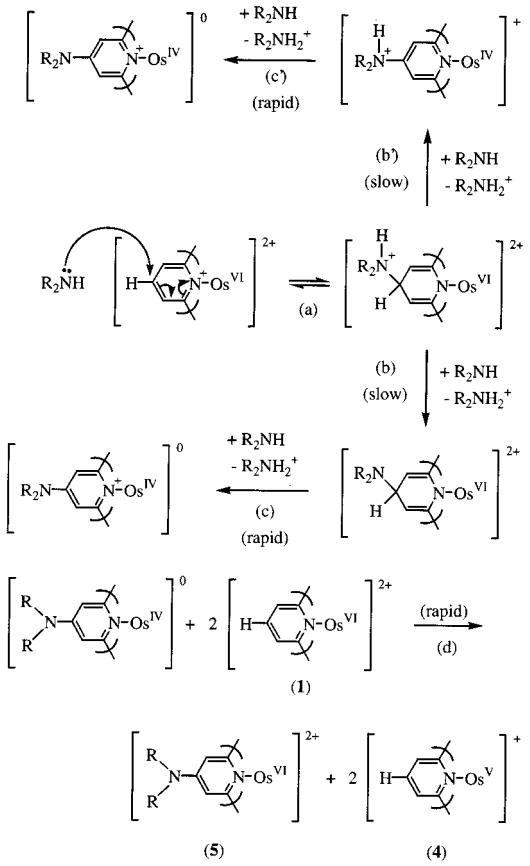

(V) and $\Delta G^\circ = -0.20$ eV for oxidation of Os(V) to Os(VI) showing that both reactions are spontaneous.

Both reactions are presumably rapid. The comproprotionation rate constant, k_{comp}, for the reaction between *trans*-$[Os^{VI}(tpy)(Cl)_2(NN(CH_2)_4O)]^{2+}$ and *trans*-$[Os^{IV}(tpy)(Cl)_2(N(H)N(CH_2)_4O)]^{+}$ in 1:60 (v/v) H_2O/CH_3CN, pH = 1, $\mu = 0.1$ M in KNO_3 is $(5.7 \pm 0.1) \times 10^6$ M^{-1} s^{-1}.[4b]

Other reasonable mechanisms can be proposed, such as initial, rapid pre-equilibrium loss of a proton to OH^- as in eq 5 or to R_2NH, followed by Os(VI → IV) intramolecular electron transfer and HNR_2 addition to the ring. Both are inconsistent with the observed rate law.

Regardless of the mechanistic details, it is apparent that Os(VI) plays a major role as a "substituent" in activating the pyridyl ring(s) toward proton loss and/or nucleophilic substitution. As illustrated in eq 5, Os(VI) stabilizes the carbanion by acting as an extraordinarily effective electron withdrawing substituent. It also provides a basis for the two-electron change that accompanies substitution based on intramolecular Os(VI) to Os(IV) electron transfer. Electron transfer is induced by nucleophilic addition to the ring followed by the amine acting as a base to remove the ring proton as in Scheme 2.

Synthesis. The mechanisms in Scheme 2 predicts a **3**:**4** ratio of 2:1 after the first addition of morpholine, Figure 4B. The yield of the morpholide-substituted complex can be made essentially quantitative by subsequent oxidation of **3** to **1** with addition of further morpholine according to eq 2.

Although the other ring-substituted products listed in Table 5 were not isolated, the implied range of reactivity by the variety of N- and O-based bases is impressive. Both primary and secondary aliphatic amines and primary aromatic amines readily react as nucleophiles, as do *tert*-butoxide, acetate,[14] and substituted pyridines. UV−vis spectra of representative alkyl amide-substituted osmium complexes are similar to the spectrum of the morpholide-substituted osmium complex (Supporting Information Figure 2).

For the complexes containing a pyridyl-substituted tpy ligand, there is evidence for pyridinium formation. Additional waves appear at low potentials in cyclic voltammograms for the $pyR^{+/0}$ couples with $E_{1/2}$(*t*-Bupy) = −1.01 V and $E_{1/2}$(2,4,6-Me_3py) = −0.87 V versus SSCE (Table 5).

As shown by the reactions between **1** and PR_3, SR_2, and the arylamines, electron transfer is a pathway in competition with oxidative substitution at tpy.[4b] The factors that dictate which of the two pathways is more facile for a given base or family of bases are unknown. They deserve further investigation since it might be possible to control the most favored pathway by varying temperature or the solvent.

In principle, nucleophilic substitution on tpy could be synthetically useful for the preparation of a variety of substituted tpy ligands. We were able to show that the tpy ligand could be removed from Os(VI) under mild basic conditions but have made no attempt to exploit this chemistry as a synthetic route for the preparation of substituted tpy ligands.

The products that result from oxidative nucleophilic substitution are highly colored with new absorption bands appearing in the region 590−636 nm (ϵ = 7740−8830 M^{-1} cm^{-1}). Examples are shown in Figure 5A and Supporting Information, Figure 2. Neglecting the pyridyl adducts, the appearance of this new absorption feature appears to depend on the presence of an electron donor substituent. It is also notable that this band shifts to higher energy for Os(V) compared to Os(VI). For **4**, λ_{max} = 624 nm and for its substituted Os(V) form, λ_{max} = 454 nm, Figure 5.

It is reasonable to assign these bands to internal ligand charge transfer (ILCT) transitions with Os(VI) (or Os(V)) acting as an electrophilic substituent, eq 6. There is a clear analogy in this assignment with transient internal charge transfer (TICT) transitions that occur in donor−acceptor aromatic molecules.[15]

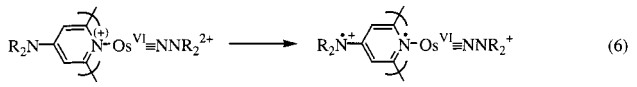

(6)

These bands may also arise from ligand-to-metal charge transfer (LMCT) transitions with the acceptor orbital largely dπ(Os(VI)) in character, eq 7.

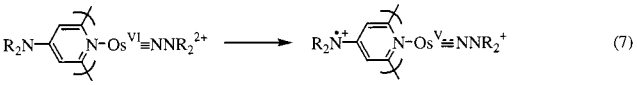

(7)

Careful inspection of the electrochemical data in Table 5 reveals that the effect of adding electron donor substituents to tpy leads to a different effect on the Os(VI/V) and Os(V/IV), Os(IV/III) couples. The difference can be explained based on a bonding model for the hydrazido complexes described earlier.[2] In this model (Scheme 3), the electronic configuration at Os(VI) is $d\delta^2$ $d\pi^*_1{}^0$ $d\pi^*_2{}^0$ with $d\pi^*_1$ and $d\pi^*_2$ largely dπ in character but antibonding because of mixing with lower lying

(14) There is no sign for the internal ligand charge transfer (ILCT) transition in the ring-substituted products that result from the K(*t*-BuOH) and $(NH_4)(COOCH_3)$.

(15) (a) Zehnacker, A.; Lahmani, F.; vanWalree, C. A.; Jenneskens, L. W. *J. Phys. Chem. A* **2000**, *104*, 1377. (b) Kobayashi, N.; Ishizaki, T.; Ishii, K.; Konami, H. *J. Am. Chem. Soc.* **1999**, *121*, 9096. (c) Ziessel, R.; Hissler, M.; ElGhayoury, A.; Harriman, A. *Coord. Chem. Rev.* **1998**, *180*, 1251. (d) Chiorboli, C.; Bignozzi, C. A.; Scandola, F.; Ishow, E.; Gourdon, A.; Launay, J. P. *Inorg. Chem.* **1999**, *38*, 2402.

Scheme 3

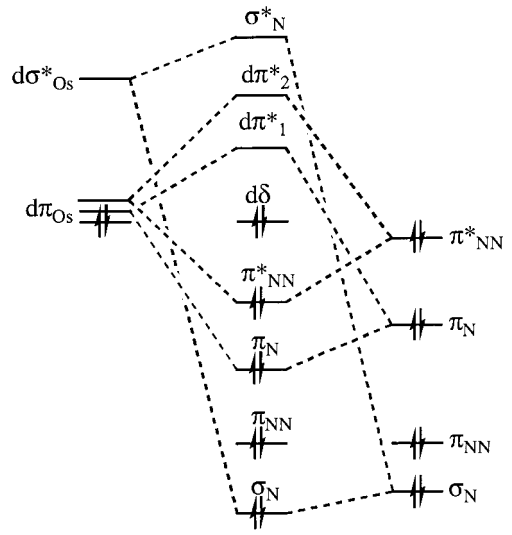

hydrazido π orbitals. dδ has delta symmetry with regard to these interactions and is a nonbonding dπ orbital.

Referring to the numbering scheme in Figure 1 and defining the *z*-axis to fall along the Os≡N bond and *yz*-plane to contain the morpholide-substituted tpy ligand in **4**, the lone pair in the p_x orbital of N(26) of the morpholide substituent is delocalized into the π-system of the tpy ligand of Os(VI). The evidence for this conclusion is in the crystallographic data. The N(26)−C(16)−C(17) angle of 121.8(5)° and N(26)−C(16)−C(15) angle of 120.6(5)° suggest sp^2-hybridization at N(26). The C(16)−C(17) bond length of 1.429(8) Å and C(16)−C(15) bond length of 1.428(8) Å are longer than C(17)−C(18) (1.372(8) Å), C(18)−C(19) (1.372(7) Å), C(19)−C(14) (1.338(7) Å), and C(14)−C(15) (1.367(8) Å). This is consistent with electronic donation from the π-electrons in N(26) to the pyridyl ring. The N(26)−C(16) bond (1.353(7) Å) is shorter than the single bonds N(26)−C(27) of 1.478(8) Å and N(26)−C(31) of 1.484(7) Å, consistent with some multiple-bonding between N(26) and C(16).

π-donation from $-NR_2$ on the tpy ligand to the unfilled dπ* levels at Os(VI) stabilize Os(VI). This decreases $E_{1/2}$Os(VI/V) from 0.98 V to ∼0.78 V (in CH_3CN, versus SSCE) for the electron donor-substituted complexes.

In oxidation states V and IV, the dπ* orbitals are singly and doubly occupied. This decreases the importance of π-donation from the remote substituents. Electronic interactions in the lower oxidation states are dominated by σ-interactions. The $-NR_2$ substituents become electron withdrawing because of the electronegativity of the donor atom. This electron withdrawing effect destabilizes oxidation states Os(V) and Os(IV) which explains the increase in $E_{1/2}$ Os(V/IV) (from 0.00 V to ∼0.15 V) and $E_{1/2}$ Os(IV/III) (from −0.79 V to approximately −0.55 V).

Acknowledgment. Acknowledgments are made to the National Science Foundation under Grant number CHE-9503738, the Los Alamos National Laboratory (DOE) under Grant Number 10730-001-00-2G, and the Laboratory Directed Research and Development Program for support of this research. My Hang V. Huynh gratefully acknowledges postdoctoral fellowship support from the Director's Office of Los Alamos National Laboratory. Los Alamos National Laboratory is operated by the University of California for the U.S. Department of Energy under Contract W-7405-ENG-36.

Supporting Information Available: Supporting Information Figures 1 and 2, Tables containing crystal data, atomic coordinates, isotropic thermal parameters, bond distances and angles, and packing diagrams. This material is available free of charge via the Internet at http://pubs.acs.org.

IC001154I